Elastic Electron-Deuteron Scattering

B. GROSSETÊTE, D. DRICKEY, AND P. LEHMANN
École Normale Supérieure, Laboratoire de l'Accélérateur Linéaire, Orsay, France

We present results on elastic electron-deuteron experiments performed at Orsay. The range of momentum transfers is 0.6 to 2 F^{-2}. Two kinds of measurements have been taken detecting the scattered electron: one with a solid CD_2 target, the other with a liquid target. The data are analyzed with the nonrelativistic theory, which gives slightly positive neutron form factors and a magnetic neutron form factor nearly equal to the magnetic proton form factor.

INTRODUCTION

THIS article describes an experiment performed with the Orsay linear accelerator in which elastic electron-deuteron scattering was studied by observing the scattered electron. We present the experimental results and attempt to clarify the theoretical results which have guided our analysis.

Elastic electron-deuteron scattering was studied for values of the four-momentum transfer q^2 less than 2 F^{-2} by observing the scattered electron. In this region, observation of the scattered electron is not only the most convenient experimental method, but also the most accurate technique to permit comparison of electron-deuteron to electron-proton scattering cross sections. The scattered electrons, being relativistic in both reactions, give identical pulse heights in the Čerenkov counter, and in addition, at low q^2 the deuteron inelastic-scattering contribution is sufficiently small to be ignored or accurately subtracted from the experimental data—especially at forward angles, where the interesting charge scattering dominates. At higher q^2, it is more precise to observe the recoil particle, thus avoiding inelastic scattering.

Our experiments at low q^2 were primarily designed to observe electric scattering and thus deduce the neutron charge form factor. However, we report in this experiment measurements of the magnetic scattering made at backward angles although they are of lesser accuracy because of the competing charge scattering.

The deuteron, being the simplest nucleus, provides the simplest target containing neutrons, and has the further advantage that the proton and neutron are only lightly bound and hence almost free. In the case of elastic electron-deuteron scattering we are concerned with the proton and neutron form factors and the binding of the proton and neutron, i.e., the deuteron wave function.

The theoretical picture of the deuteron is not perfect at present. At low q^2 the scattering probes only the exterior of the deuteron and one has nonrelativistic theories available for the analysis. One has a certain confidence in these theories since they describe adequately the static properties of the deuteron (except the magnetic moment) and the order of magnitude of corrections to the theory seems to be small. It is well known that these nonrelativistic theories are only slightly sensitive to the inner form of the potential at low q^2.

For example, the calculation of the deuteron charge form factor is known to a few percent, the relativistic corrections being of the order of $q^2/4M^2$ (1% at $q^2=1$ F^{-2}) although it must be added that the exchange-current corrections are unknown.[1,2] The magnetic form factor is less certain than the electric form factor because even at $q^2=0$ the presently accepted models of the deuteron with 7% D state do not explain the static magnetic moment μ_d, the error being about 4%. We feel that the theory for the electric scattering can be theoretically described with an error of the same order as our experimental error in this q^2 range, i.e., 1–3%. A better description of the deuteron would allow convincing conclusions about the neutron-charge form factor from these measurements.

Because the interpretation of these experiments is rather difficult, we have felt it necessary to enumerate carefully both the experimental errors and the theoretical uncertainties. Consequently we present a rather lengthy reformulation of the theoretical picture in this article.

I. THEORY OF ELASTIC SCATTERING

The first discussion of elastic electron-deuteron scattering was the nonrelativistic theory given by Jankus.[3] A relativistic description was first studied by Glaser and Jaksic,[4] who demonstrated the existence of three form factors for the deuteron.

The Breit frame proves to be convenient for comparing the nonrelativistic theories with the general relativistic form. We can more easily separate the fundamental hypotheses (such as one-photon exchange, and the fact that the deuteron has spin 1) and the various approximations one is forced to make. This formulation has already been partly published, but it seems essential to us to assemble the results obtained by various authors and to clarify a certain number of details.

A. The Relativistic Expression for the Cross Section

(a) *One-Photon Exchange*

The fundamental hypothesis used in the calculation is the validity of the first Born approximation, corre-

[1] J. Ginibre (private communication).
[2] R. J. Adler and S. D. Drell, Phys. Rev. Letters **13**, 349 (1964).
[3] V. Z. Jankus, Phys. Rev. **102**, 1586 (1956).
[4] V. Glaser and B. Jaksic, Nuovo Cimento **5**, 1197 (1957).

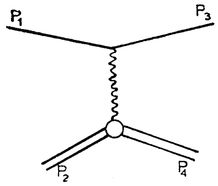

FIG. 1. Feynman diagram of an elastic scattering of electrons using the first Born approximation.

sponding to a single photon exchanged between the electron and deuteron currents (Fig. 1). This hypothesis has been well verified for the proton at low q^2,[5,6] although there is some evidence for small deviations near $q^2=20$ F^{-2}.[7,8] We assume that these results apply to the deuteron as well.

With this hypothesis, Gourdin and Martin[9] have shown the general form for the cross section for electron scattering on a particle of any spin to be

$$\frac{d\sigma}{d\Omega}=\frac{e^2}{4}\frac{1}{p_{01}{}^2}\frac{p_{03}}{p_{01}}\frac{\cos^2(\theta/2)}{\sin^4(\theta/2)}[A(q^2)+B(q^2)\tan^2(\theta/2)], \quad (1)$$

where p_{01} and p_{03} are the incident and scattered electron energies, and θ is the scattering angle. The expression for the cross section contains only two functions of the invariant momentum transfer.

(*b*) *Deuteron Form Factors*

The expressions for $A(q^2)$ and $B(q^2)$ depend on the current of the particle scattering the electron. For spin 0 we have only one invariant quantity to consider, spin $\frac{1}{2}$ gives two, and spin 1 gives three. This last case can most easily be demonstrated in the Breit frame[10] where

$$\mathbf{p}_2=-\mathbf{p}_4=-\mathbf{q}/2, \quad (2)$$

$$p_{02}=p_{04}, \quad (3)$$

$$q_4=0. \quad (4)$$

Denote by $\Gamma_{\lambda'\lambda}{}^{\mu}$ the μ component of the current between the helicity states λ and λ'. Application of the conservation of electromagnetic current, time reversal, and symmetry with respect to the plane (103) leads to the following properties:

The component 3 is proportional to the component 0, the components 0, $+1$, -1 being represented by the following tables as a function of helicity:

For $\Gamma_{\lambda'\lambda}{}^0$:

λ' \ λ	-1	0	1
-1	0	0	$b(q^2)$
0	0	$a(q^2)$	0
1	$b(q^2)$	0	0

For $\Gamma_{\lambda'\lambda}{}^+=(\Gamma_{\lambda'\lambda}{}^1+i\Gamma_{\lambda'\lambda}{}^2)/\sqrt{2}$:

λ' \ λ	-1	0	1
-1	0	$c(q^2)$	0
0	0	0	$-c(q^2)$
1	0	0	0

For $\Gamma_{\lambda'\lambda}{}^-=(\Gamma_{\lambda'\lambda}{}^1-i\Gamma_{\lambda'\lambda}{}^2)/\sqrt{2}$:

λ' \ λ	-1	0	1
-1	0	0	0
0	$-c(q^2)$	0	0
1	0	$c(q^2)$	0

Thus we are led to three quantities (or form factors) which are functions solely of q^2.

Grossetête and Lehmann[11] and, more systematically, Gourdin[12] have introduced three form factors for the deuteron with a simpler normalization than in older forms. These are G_{Ed}, the charge form factor; G_{Qd}, the quadrupole form factor; and G_{Md}, the magnetic form factor. At $q^2=0$ the normalizations are

$$G_{Ed}(0)=1, \quad (5)$$

$$G_{Qd}(0)=Q, \quad (6)$$

where $Q=24.8$ is the deuteron quadrupole moment in units of $e/M_d{}^2$, and

$$G_{Md}(0)=\mu_d, \quad (7)$$

where $\mu_d=1.713$ is the magnetic moment in units of $e/2M_d$.

In the Breit frame the form factors are expressed in terms of the matrix elements as

$$G_{Ed}=\frac{M_d}{p_{02}}\frac{\sum_\lambda \Gamma_{-\lambda\lambda}{}^0}{3e}, \quad (8)$$

$$G_{Qd}=\frac{2M_d{}^2}{q^2}\frac{M_d}{p_{02}}\frac{(\Gamma_{00}{}^0-\Gamma_{-11}{}^0)}{e}, \quad (9)$$

and

$$G_{Md}=\frac{2M_d}{q}\frac{M_d}{p_{02}}\frac{\Gamma_{0-1}{}^+}{e}. \quad (10)$$

[5] B. Dudelzak and P. Lehmann, in *Proceedings of the Sienna International Conference on Elementary Particles, 1963*, edited by G. Bernadini and G. P. Puppi (Società Italiana di Fisica, Bologna, 1963), Vol. 1, p. 495.

[6] Robert R. Wilson and Joseph S. Levinger, Ann. Rev. Nucl. Sci. **14**, 135 (1964).

[7] J. C. Bizot, J. M. Buon, J. Perez-y-Jorba, and Ph. Roy, Phys. Rev. Letters **11**, 480 (1963).

[8] A. Browman and J. Pine, in *Nucleon Structure, Proceedings of the International Conference at Stanford University, 1963*, edited by R. Hofstadter and L. I. Schiff (Stanford University Press, Stanford, California, 1964).

[9] M. Gourdin and A. Martin, CERN Report (unpublished).

[10] Loyal Durand, III, Paul C. De Celles, and Robert B. Marr, Phys. Rev. **126**, 1882 (1962).

[11] B. Grossetête and P. Lehmann, Nuovo Cimento **28**, 423 (1963).

[12] M. Gourdin, Nuovo Cimento **28**, 533 (1963); **32**, 493 (1964).

(c) *Differential Cross Section*

The differential cross section can be written, in a form not involving cross terms, in terms of the preceding functions.

$$\frac{d\sigma}{d\Omega}=\sigma_{\text{Mott}}\frac{1}{3e^2}\left\{\sum_{\lambda\lambda'}\frac{(\Gamma_{\lambda'\lambda}{}^0)^2+(\Gamma_{\lambda'\lambda}{}^+)^2}{1+q^2/4M_d{}^2}+2\tan^2(\theta/2)\sum_{\lambda\lambda'}(\Gamma_{\lambda'\lambda}{}^+)^2\right\}, \tag{11}$$

$$\sigma_{\text{Mott}}=\frac{\alpha^2}{4p_{01}{}^2}\frac{\cos^2(\theta/2)}{\sin^4(\theta/2)}\frac{1}{1+(2p_{01}/M_d)\sin^2(\theta/2)}. \tag{12}$$

In this expression the normalization of the density of states in momentum space is

$$(M_d/p_{02})d^3p/(2\pi)^3.$$

Since

$$\sum_{\lambda\lambda'}(\Gamma_{\lambda'\lambda}{}^0)^2=\Gamma_{00}{}^{02}+2\Gamma_{-1\,1}{}^{02}$$
$$=\tfrac{1}{3}(\Gamma_{00}{}^0+2\Gamma_{-1\,1}{}^0)^2+\tfrac{2}{3}(\Gamma_{00}{}^0-\Gamma_{-1\,1}{}^0)^2, \tag{13}$$

and

$$\sum_{\lambda\lambda'}(\Gamma_{\lambda'\lambda}{}^+)^2=2(\Gamma_{-10}{}^+)^2, \tag{14}$$

the cross section is given by

$$\frac{d\sigma}{d\Omega}=\sigma_{\text{Mott}}\left\{G_{Ed}{}^2(q^2)+\frac{q^4}{18M_d{}^4}G_{Qd}{}^2(q^2)+\frac{q^2}{6M_d{}^2}G_{Md}(q^2)\left[1+2\left(1+\frac{q^2}{4M_d{}^2}\right)\tan^2(\theta/2)\right]\right\}, \tag{15}$$

which is an expression very similar to that for the proton:

$$\frac{d\sigma}{d\Omega}=\sigma_{\text{Mott}}\left\{\frac{G_{Ep}(q^2)+(q^2/4M^2)G_{Mp}{}^2(q^2)}{1+q^2/4M^2}+\frac{2q^2}{4M^2}G_{Mp}{}^2(q^2)\tan^2(\theta/2)\right\}, \tag{16}$$

where M is the proton mass and G_{Ep} and G_{Mp} are the electric and magnetic form factors of the proton—the essential difference being $1+q^2/4M^2$, which corresponds to the relativistic contraction $p_0{}^2/M^2$. In the case of the proton, the proton current contains only two invariants, permitting one to separate the two invariant functions in the cross-section expression using the angular dependence. For the deuteron, on the other hand, there are three invariant quantities, and a complete separation can be made only by analyzing the polarization of the scattered particle.

B. Calculation of the Deuteron Form Factors

The nuclear physics in elastic electron-deuteron scattering problems is introduced in the deuteron form factors. The problem becomes essentially a three-body problem when the neutron and proton bound within the deuteron are introduced, and one is thus led to approximations to find a solution. Since the nucleons are only weakly bound, the impulse approximation should be valid and one can consider the proton and neutron to be on the mass shell both in their interaction with the virtual γ ray and in the nucleon propagator.

Using these two hypotheses, the deuteron form factors may be written as the product of the nucleon isoscalar form factors with a function of q^2 which depends on the deuteron's structure:

$$G(q^2)=[G_p(q^2)+G_n(q^2)]g(q^2). \tag{17}$$

At present no relativistic treatment of the deuteron is known and we must limit ourselves to the nonrelativistic case in analyzing our experimental results.

(a) *Nonrelativistic Approximations*

The nonrelativistic theory was first elaborated by Jankus[3] who considered only point nucleons. One could, as Kramer and Glendenning[13] did, introduce immediately the nucleon form factors by applying Eq. (17). We prefer another presentation because it demonstrates the simplicity of the Breit system in the calculation. In Sec. IA it was shown that the form factors appear naturally in the relativistic formulation in the Breit system. In the nonrelativistic treatment two additional advantages appear: The four-momentum and three-momentum transfers are identical (thus eliminating a certain number of uncertainties in applying these quantities), and a more physical interpretation of the form factors becomes apparent.

In fact we can apply the same interpretation to the deuteron which Sachs[14] applied to the proton, and consider the 0 component of the current in the Breit frame as the Fourier transform of the charge distribution while the other components can be considered as the Fourier transform of the current distribution. Supposing the nucleons to be free in the deuteron, the distribution of charge (current) is the convolution of the distribution of the nucleons in the deuteron with their distribution of charge (current) given by Sachs's form factors.

$$\frac{\Gamma_{\lambda\lambda'}{}^0}{(1+q^2/4M_d{}^2)^{1/2}}=e\left|\int\psi_{-\lambda'}{}^*(\mathbf{x})e^{i\mathbf{q}\cdot\mathbf{x}/2}\psi_\lambda(\mathbf{x})d^3x\right|[G_{Ep}(q^2)+G_{En}(q^2)], \tag{18}$$

[13] Norman K. Glendenning and Gustav Kramer, Phys. Rev. **126**, 2159 (1962).
[14] R. G. Sachs, Phys. Rev. **126**, 1365 (1962).

$$\frac{\mathbf{\Gamma}_{\lambda\lambda'}}{(1+q^2/4M_d^2)^{1/2}}=\frac{ie}{2M}\int\psi_{-\lambda'}{}^*(\mathbf{x})\bigg(e^{i\mathbf{q}\cdot\mathbf{x}/2}\mathbf{q}\times[G_{Mp}(q^2)\boldsymbol{\sigma}_p+G_{Mn}(q^2)\boldsymbol{\sigma}_n]+[e^{i\mathbf{q}\cdot\mathbf{x}/2},\mathbf{q}\times\mathbf{L}]_+\frac{G_{En}(q^2)+G_{Ep}(q^2)}{2}\bigg)\psi_\lambda(\mathbf{x})d^3x\,, \quad (19)$$

where $\psi_\lambda(\mathbf{x})$ is the deuteron wave function.

The symmetrization of the convection term in the spatial part of the current is the analog of that normally done with a nonrelativistic Hamiltonian.

We use the nonrelativistic wave function of the deuteron

$$\psi_\lambda(x)=\frac{1}{(4\pi)^{1/2}}\frac{1}{r}\bigg[u(r)+\frac{S_{np}}{2\sqrt{2}}w(r)\bigg]\chi_{1\lambda}\,, \quad (20)$$

$\chi_{1\lambda}$ being the triplet spin function, and the calculation leads to the following expressions for the deuteron form factors:

$$G_{Ed}(q^2)=(G_{Ep}+G_{En})\int_0^\infty(u^2+w^2)j_0(qr/2)dr\,, \quad (21)$$

$$\frac{q^2}{(18)^{1/2}M_d^2}G_{Qd}(q^2)=(G_{Ep}+G_{En})\int_0^\infty 2\bigg(uw-\frac{w^2}{2\sqrt{2}}\bigg)j_2(qr/2)dr\,, \quad (22)$$

$$G_{Md}(q^2)=\frac{M_d}{M}\int_0^\infty\{[(G_{Mp}+G_{Mn})(u^2+w^2)-\tfrac{3}{2}(G_{Mp}+G_{Mn}-\tfrac{1}{2}(G_{Ep}+G_{En}))w^2]j_0(\tfrac{1}{2}qr)+[(1/\sqrt{2})(G_{Mp}+G_{Mn})w(u+(1/\sqrt{2})w)-\tfrac{3}{16}(G_{Ep}+G_{En})w^2]j_2(\tfrac{1}{2}qr)\}dr\,. \quad (23)$$

The wave functions u and w have generally been calculated from a potential

$$V(r)=V_c(r)+V_t(r)S_{np}+V_{LS}\mathbf{S}\cdot\mathbf{L} \quad (24)$$

containing three terms: central, tensor, and spin-orbit.

(b) *Choice of a Nonrelativistic Potential*

At large distances the wave function of the deuteron is determined by the one-pion-exchange potential (OPEP). At smaller distances the potential has to describe adequately the static properties of the deuteron (binding energy, quadrupole moment, effective range) as well as proton-neutron scattering results (triplet scattering length, neutron-proton phase shifts).

To analyze our results we have chosen the potential of Glendenning and Kramer (No. 8)[13] and that of Hamada.[15] In Table I we give some of their properties. Both these potentials have a hard core of about 0.5 F, as is shown to be needed by neutron-proton scattering experiments at high energy and by electron-deuteron experiments. At sufficiently low q^2 the electron-deuteron scattering results are, to a certain extent, independent of these potentials ($\approx 1\%$ difference at $q^2=2.5$ F^{-2}).

The major failure of the nonrelativistic theory is that the 6–7% D state found to be necessary in these potentials leads to an incorrect value of the deuteron magnetic moment (4% D state would be necessary). One finds a large D state because in attempting to explain Q one is led to a constant asymptotic value of the ratio of u and w and roughly a constant percentage of D state, in turn because the nucleons are essentially outside the range of the nuclear force. The deuteron magnetic moment is thus not explained by a nonrelativistic theory and the magnetic form factor at $q^2=0$ is too low. One could, of course, normalize the calculation at $q^2=0$ as suggested by Gourdin and assume the variation as a function of q^2 to be small.

Gourdin[12] has discussed the various approximations in the nonrelativistic theory using a current similar to Eqs. (25) and (26) and performing the calculation in the Breit system. We list these approximations briefly here:

$$j_0=eG_{Ed}(q^2)\chi_{s'}{}^*\chi_s\,, \quad (25)$$

$$\mathbf{j}=(ie/2M)[G_{Md}(q^2)\chi_{s'}{}^*(\boldsymbol{\sigma}\times\mathbf{q})\chi_s-G_{Ed}(q^2)P\chi_{s'}{}^*\chi_s]\,, \quad (26)$$

P being the sum of the moments of the two nucleons.

The impulse approximation is used. The fact that the Breit frames for the nucleons and the deuteron do not coincide leads to the introduction of terms proportional to the momentum of the spectator nucleon. After taking this step we arrive at expressions identical to those of Jankus, except for a singlet and negligible discrepancy in the orbital part of G_{Md}.

The introduction of the form factors of the free nucleons assumes the nucleons to be on the mass shell. The wave function used is nonrelativistic, and finally one assumes no retardation in the calculation of the interaction with the photon.

[15] E. F. Erickson (private communication).

TABLE I. Properties of the potentials of Glendenning and Kramer (No. 8) and of Hamada.

Potential	Quadrupole moment Q (10^{-27} cm²)	Triplet scattering length a_t (F)	D-state contribution P_D	Hard-core radius r_c (F)	Strong-interaction constant (units of F²/4M)	Deuteron effective range r_t^d (F)
Glendenning-Kramer, No. 8	2.818	5.413	0.0562	0.50	0.08	
Hamada	2.840		0.072	0.50		1.752
Experimental values	2.82±0.02	5.396±0.011				

(c) *Relativistic Theories*

We list briefly the various relativistic calculations known to us in an attempt to show their effects on our data.

The major effort to date has been an attempt to calculate the relativistic wave function of the deuteron. Blankenbecler[16] has used a model of the deuteron consisting of two bosons, and finds a smaller cross section than that given by the nonrelativistic formulation. Jones[17] uses the "tail approximation" and compares a relativistic treatment with a nonrelativistic one where the wave function is reduced to its asymptotic form. He finds correction terms of the order $[1+(q^2/4M^2)]^{-1}$ which reduce the cross section.

Tran Thanh Van[18] has performed a more complete calculation. He has attempted to correct the "mass-shell" approximation by using three different expressions for the nucleon propagator. The deuteron model consists of two fermions. At low q^2 and for the $q^2=0$ normalization he uses the Born approximation in the neutron-proton-deuteron vertex, and at higher transfers he takes the separable-nucleus approximation. Contrary to the other theories, he finds a larger cross section than that given by the nonrelativistic theory. He uses a generalization of the Hulthén wave function, and use of a more complicated neutron-proton vertex may soon produce more believable results.

Since these theories lead to contradictory results, we are forced to use the nonrelativistic theory for our analysis. One might hope that the situation will clarify with the extension of Tran's work and with a recent calculation of Drell[2] which seems to connect the habitual assumption of 7% D state with the static deuteron magnetic moment.

II. EXPERIMENTAL MATTERS: MEASUREMENT OF ELASTIC SCATTERING BY OBSERVATION OF THE RECOIL ELECTRON

A. General Considerations

(a) *Electric Scattering*

It is an obvious fact that of the signs of the four nucleon form factors, only that of G_{En} is undetermined by the $q^2=0$ normalization. In practice this normalization is taken from the measurements of the neutron-electron interaction[19] which gives the result

$$(dG_{En}/dq^2)_{q^2=0}=0.021\pm0.001\,, \tag{27}$$

and predicts positive values for G_{En} at low q^2. Since these measurements were taken at extremely small values of momentum transfer, it is highly desirable to make measurements at a larger q^2 to confirm these measurements, and to determine the behavior of G_{En} as a function of q^2. A guide to the magnitude of the effect one might expect is given by the fact that any dispersion-theory fit of the form factors shows that little curvature can exist in the form factors unless a very low mass state is present. Since at present the ρ, ω, and ϕ vector mesons have the lowest masses among particles thought to influence the form factors, we can say that G_{En} must be linear at sufficiently low q^2 and that the curvature of G_{En} is small around $q^2=1$ F^{-2} (a value of 10^{-2} for the coefficient of the second order of the expansion in q^2). Thus one expects to find very small values for G_{En} compared with those of G_{Ep} (a few percent). To observe such a small parameter it seems necessary either to observe it directly or to observe the interference term between it and another large term. Furthermore the interference term permits a determination of the sign of G_{En} if the sign of the dominant term is known. This is precisely the case in elastic electron-deuteron scattering, where the charge scattering is proportional to $(G_{Ep}+G_{En})^2$, whereas in elastic scattering, it is proportional to $G_{Ep}^2+G_{En}^2$, and in a coincidence experiment between the scattered electron and recoil neutron, to G_{En}^2.

Sufficiently accurate cross sections should then determine G_{En} at q^2 of the order of 1 F^{-2} if G_{Ep} is known.

In this series of experiments we have made two types of measurements in the range $q^2=0.6$ F^{-2} to $q^2=1.9$ F^{-2}. The first used a deuterated polyethylene target and gave absolute electron-deuteron cross sections. The measurements were performed during the same period and with the same apparatus as Dudelzak and Lehmann's proton measurements.[20] In the interpretation we used their proton form factors in order to cancel many errors. The cross sections have been measured

[16] R. Blankenbecler, Ph.D. thesis (unpublished).
[17] H. F. Jones, Nuovo Cimento **26**, 790 (1962).
[18] J. Tran Thanh Van, thesis, Orsay, 1963 (unpublished); Ann. Phys. (Paris) **9**, 139 (1963).
[19] For a review of this, see Leslie L. Foldy, Rev. Mod. Phys. **30**, 471 (1958).
[20] B. Dudelzak, G. Sauvage, and P. Lehmann, Nuovo Cimento **28**, 18 (1963).

TABLE II. Deuteron absolute cross sections from the CD_2 measurements.

q^2 (F^{-2})	θ (deg)	p_{01} (MeV)	$d\sigma/d\Omega$ (10^{-32} cm^2)
0.882	60	189.9	59.4 ±1.8
0.998	60	202.4	44.7 ±1.6
1.001	90	144.8	14.63 ±0.28
1.009	130	114.7	3.241±0.095
1.352	60	236.5	22.91 ±0.76
1.350	60	236.3	23.89 ±0.76
1.334	110	146.2	3.78 ±0.11

several times, for both deuteron and proton data, at three-month intervals, and the reproducibility is satisfactory. On the other hand Dudelzak and Lehmann have repeated their measurements at $q^2=1$ F^{-2} in another experimental area and have found good agreement.[21]

The second deuteron measurement is a direct ratio measurement using a liquid target containing either hydrogen or deuterium. We measure a cross-section ratio proportional to $(1+G_{En}/G_{Ep})^2$. Our results for G_{En} are presented below using, as discussed in the preceding theoretical section, our best choice of a nonrelativistic potential to describe the intrinsic deuteron physics of the problem.

(b) *Magnetic Scattering*

We present below in addition to electric scattering measurements, measurements at backward angles where we have extracted the magnetic scattering from the deuteron. Although probably on less firm theoretical grounds, we have nevertheless used the nonrelativistic deuteron model to determine the neutron magnetic form factor at $q^2=1.0$, 1.35, and 1.9 F^{-2}.

B. Experimental Methods

Scattering of energy-analyzed incident electrons coming from the Orsay linear accelerator was observed by analyzing recoil electrons using a double-focusing spectrometer and counting them in a Lucite Čerenkov counter. Variable momentum-analyzing slits placed before the Čerenkov counter permitted selection of momentum resolution to minimize observation of inelastic scattering events coming from deuteron breakup.

Some counts from inelastic events were observed, and a correction for these events was deduced either by using the elastic peak to simulate the inelastic continuum or by observing the shape of the elastic and inelastic scattering using very narrow momentum resolution. This correction was practically zero ($<0.2\%$) except for some backward-angle measurements.

Beam currents were monitored with an integrator and calibrated capacitor using a secondary emission monitor placed after the target and frequently calibrated against a Faraday cup.

[21] B. Dudelzak, thesis, Orsay Linear Accelerator Laboratory Report No. 1127 (unpublished).

With the liquid target and for some points a small correction ($<0.5\%$) was necessary for electrons multiply scattered out of the Faraday cup, but this source of error was suppressed in the ratio of the deuteron and proton cross sections. With the solid target, and for very low incident energy of the electrons, we placed some of the apparatus in a helium atmosphere in order to eliminate this effect.

Counts were recorded on a pulse-height analyzer, and the counter efficiency and counting-rate correction were deduced in the standard manner.[22,23]

The "flat-top" method was used—i.e., the spectrometer resolution was chosen to be larger than the elastic peak width—as being the method least sensitive to minor energy variations. Nevertheless the narrow resolution, dictated by the necessity to avoid inelastic events, was sensitive to energy shifts. Accordingly, before and after each run (every three hours) the energy was checked by changing the spectrometer to the "flat-top" edge where the counting rate is an extremely sharp function of energy. A point was rejected when an unacceptable deviation was observed. This did not occur during normal operation of the accelerator.

Beam position was continuously monitored with a zinc sulfite screen and remote television. The spectrometer's solid angle was limited by slits placed at its entrance, and scattered electron energy as measured by the spectrometer was used to calculate the incident energy, the spectrometer being previously calibrated with a floating wire. Two calibrations at a two-year interval differ by 0.5% and are in agreement with an α-particle measurement to within 0.5%. Thus we suppose an uncertainty of 0.5% in the spectrometer calibration.

C. Targets

We have used two different types of targets, the first being suited to absolute measurements, the second to taking ratios. The solid CD_2 target used for absolute cross sections was ≈ 1 mm thick, the deuterium content being 98.31% and the remaining 1.69% of hydrogen being kinematically eliminated from contributing counts. The carbon contribution of about 30% of the total was subtracted by using a carbon target of known thickness. This subtraction was also checked by measuring the elastic peak of carbon with both the CD_2 and the C target. When in use, the target was moved continually up and down by a pneumatic system, thus minimizing local heating and radiation effects and local thickness variations ($<1\%$).

The small target length permitted absolute cross-section measurements, but the solid target limited the q^2 range available: for $q^2<0.7$ F^{-2} the elastic carbon and deuteron peaks were too close together to allow use of

[22] P. Lehmann, R. Taylor, and Richard Wilson, Phys. Rev. **126**, 1183 (1962).

[23] D. Treille, Orsay, Linear Accelerator Laboratory Report No. 1044, 1962 (unpublished).

TABLE III. CD_2 results: G_{En} using Hamada or Glendenning-Kramer (GK) potential and proton form factors from Orsay or Stanford.

q^2 (F^{-2})	$G_{Ed}^2+(q^4/18M_d^4)G_{Qd}^2$ experimental	G_{Ep} Orsay	G_{Ep} Stanford	$G_{Ed}^2+(q^4/18M_d^4)G_{Qd}^2$ $(G_{Ep}+G_{En})^2$ calculated with GK potential	$G_{Ed}^2+(q^4/18M_d^4)G_{Qd}^2$ $(G_{Ep}+G_{En})^2$ calculated with Hamada potential	$1+G_{En}/G_{Ep}$ with GK potential	G_{En} with GK potential	$1+G_{En}/G_{Ep}$ with Hamada potential	G_{En} with Hamada potential	using G_{Ep} from
0.882	0.354	0.894	0.909	0.4114	0.4156	1.037	0.033±0.013	1.033	0.029±0.013	Orsay
						(1.021)	(0.019)	(1.015)	(0.014)	Stanford
1.000	0.3052	0.881	0.898	0.3766	0.3789	1.022	0.020±0.008	1.019	0.017±0.008	Orsay
						(1.003)	(0.003)	(1.000)	(0.000)	Stanford
1.351	0.221	0.845	0.865	0.2906	0.2925	1.032	0.027±0.009	1.028	0.024±0.009	Orsay
						(1.008)	(0.007)	(1.005)	(0.004)	Stanford

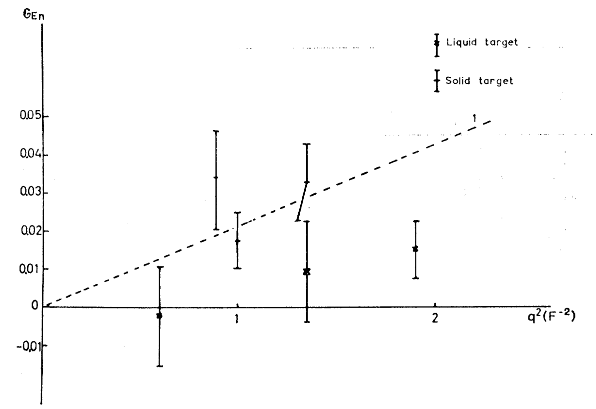

FIG. 2. G_{En} calculated with the Glendenning-Kramer No. 8 potential. For the solid target the proton form factors are Dudelzak's (Ref. 20).

the flat-top method, and for $q^2>1.4$ F^{-2} the carbon inelastic scattering became too large compared with the diminishing deuteron elastic peak.

To increase the available q^2 range and to diminish the background subtraction, we have used a liquid target permitting condensation of either hydrogen or deuterium. Because of the thickness of the target, its effective length at some angles was defined by the spectrometer optics and absolute measurements were not possible. Consequently we have measured ratios of deuterium to hydrogen cross sections, either at constant q^2 or at constant recoil electron energy. As pointed out previously, it is precisely this ratio which is interesting. The target was of the condensation type, an aluminum cylinder 2.2 cm in diameter by 10 cm long with 0.004-cm walls, whose axis was oriented either at 30° to the incident beam or perpendicular. Target temperature was monitored to ±0.1° by observing the vapor pressure of liquid hydrogen in small "bulbs" placed at each end of the cylinder and surrounded by the liquid in the cell. We observed the temperature to be 0.1° above that of the hydrogen reservoir and to be negligibly dependent on incident-beam intensity. Hydrogen density was taken as 0.0700 g/cm³ and deuterium density as 0.1691 g/cm³. We point out that the ratio of densities in practically temperature-independent in this region. The deuterium or hydrogen gas was purified by passing it through an activated-charcoal trap refrigerated with liquid nitrogen before each condensation. The target could be emptied easily for empty-target runs, using a similar trap to evacuate the liquid and pumping the residual gas with a vacuum pump.

III. ANALYSIS AND EXPERIMENTAL RESULTS

A. Absolute Cross Sections

Table II lists our measured absolute cross sections using the CD_2 target. Using the angular distribution measured at $q^2=1$ F^{-2}, we have analyzed directly to find the deuteron magnetic form factor G_{Md}. This

TABLE IV. Liquid-target ratio cross sections.

θ (deg)	$(p_{01})_d$ (MeV)	$(q^2)_d$ (F^{-2})	$(p_{01})_p$ (MeV)	$(q^2)_p$ (F^{-2})	$(d\sigma/d\Omega)_d / (d\sigma/d\Omega)_p$
65	146.1	0.606	146.7	0.588	0.506 ±0.012
70	203.1	1.302	217.3	1.386	0.323 ±0.007
135	134.4	1.411	134.6	1.277	0.1427±0.0040
85	210.8	1.890	234.1	2.094	0.2193±0.0053
85	210.8	1.890	222.9	1.915	0.1911±0.0046
135	163.3	2.037	160.9	1.756	0.0761±0.0024
145	155.4	1.963	154.7	1.720	0.0666±0.0027

TABLE V. Liquid target: $[(d\sigma/d\Omega)/\sigma_{\text{Mott}}]_d/G_{Ep}^2$ against the angle, at constant q^2. To have the same q^2 values we made interpolations.

q^2 (F^{-2})	θ (deg)	$[(d\sigma/d\Omega)/\sigma_{\text{Mott}}]_d / G_{Ep}^2$
1.964	85	0.210
	135	0.228
	145	0.257
1.351	70	0.303
	135	0.331
0.606	65	0.523

separation of electric and magnetic scattering gives the result:

$$G_{Ed}^2+(q^4/18M_d^4)G_{Qd}^2=0.3052\pm0.0086\,,$$
$$G_{Md}^2=2.088\pm0.66\,,$$

and

$$(G_{Md}/\mu_d G_{Ed})=1.530\pm0.260\,,$$

at $q^2=1.0$ F^{-2}.

Given these cross sections one can deduce the neutron magnetic and charge form factors using known proton form factors and a model for the deuteron. We have chosen to use the potential 8 of Glendenning and Kramer or the Hamada potential for the deuteron, and the measurements of Dudelzak[20] for the proton form factors. Three different measurements of the proton form factors, sufficiently accurate to be useful for this analysis, are known to us. They are those of Dudelzak, Drickey, and Hand[24] and of Frèrejacque.[25] The differences in these measurements, though slight, are large enough to influence our analysis; in particular the G_{Ep} values of the second reference are a few percent larger than those of Dudelzak[26] (Table III), and hence lead to smaller values of G_{En}; the values of G_{Ep} in the third reference lie between the other two. Our choice is based on the fact that we attempt as nearly as possible to choose values which give the ratio of deuterium to hydrogen cross sections, hoping thereby to minimize systematic errors; the methods used in the Dudelzak measurements are nearly identical to ours. In particular the same spectrometer, solid angle, Čerenkov counter, beam monitors, and carbon target for background subtractions were used in the two experiments, the only major difference being in the choice of larger resolution in the proton measurements.

Using these measurements with the Glendenning-Kramer and Hamada potentials we find for G_{En} the result shown in Fig. 2 and Table III.

B. Ratio Measurements

Using the liquid target, we have measured the ratio of elastic deuteron to elastic proton scattering cross sections at constant angle and either constant q^2 or constant scattered electron energy, the latter being chosen at times to check that there were no uncertainties in the magnet optics. The experiment was performed as nearly as possible as a ratio measurement, the same target, counter, counting apparatus, and, in particular, the same spectrometer resolution being used for both deuterium and hydrogen measurements, the radiative corrections cancelling to good accuracy in the ratio. We find the ratios given in Tables IV and V.

The electric scattering has been analyzed to determine G_{En} using the Glendenning-Kramer potential No. 8 and the Hamada potential, as shown in Fig. 2 and Table VI. In this analysis we use only the forward-angle points, correcting for the proton magnetic scattering using $G_{Mp}=\mu_p G_{Ep}$, well verified at low q^2, and $G_{Md}=\mu_d G_{Ed}$, a minor correction sufficiently well verified by our backward-angle measurements. We have corrected the proton form factors to the same q^2 as for the deuteron measurements, this correction introducing a negligible error.

The cross-section ratios at backward angles have been

TABLE VI. Liquid-target results: G_{En} using Hamada or Glendenning-Kramer (GK) potential.

q^2 (F^{-2})	$[G_{Ed}^2+(q^4/18M_d^4)G_{Qd}^2]/G_{Ep}^2$ Experimental	$[G_{Ed}^2+(q^4/18M_d^4)G_{Qd}^2]/G_{Ep}^2$ Calculated with GK potential	$[G_{Ed}^2+(q^4/18M_d^4)G_{Qd}^2]/G_{Ep}^2$ Calculated with Hamada potential	$1+G_{En}/G_{Ep}$ with GK potential	$1+G_{En}/G_{Ep}$ with Hamada potential	G_{En} with GK potential	G_{En} with Hamada potential
0.606	0.523	0.5227	0.5269	0.997	0.994	−0.003±0.014	−0.006±0.014
1.351	0.297	0.2906	0.2925	1.011	1.008	0.009±0.014	0.006±0.014
1.964	0.203	0.1950	0.1962	1.020	1.017	0.015±0.008	0.012±0.008

[24] D. J. Drickey and L. N. Hand, Phys. Rev. Letters **9**, 521 (1962).
[25] D. Frèrejacque, D. Benaksas, and D. Drickey, Phys. Letters **12**, 74 (1964).
[26] The measurements of Refs. 24 and 20 were taken for different q^2 values than those of our deuteron experiment. The proton form factors we use are obtained by making a second-order q^2 expansion with the least-square method applied to the experimental form factors to 2 F^{-2}.

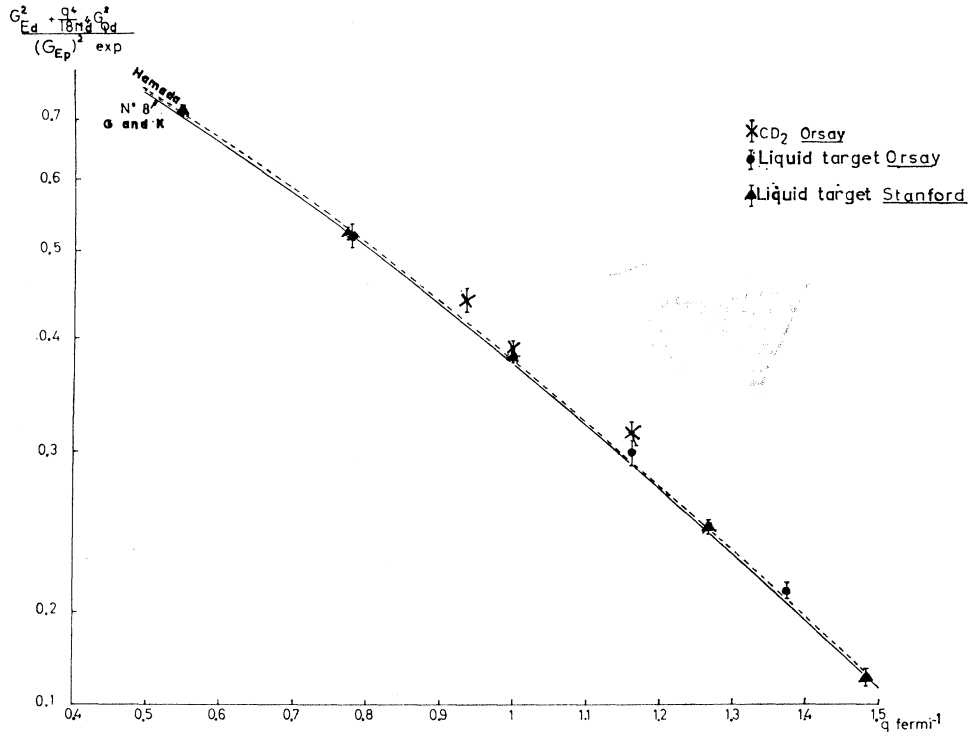

FIG. 3. $[G_{Ed}^2+(q^4/18M_d^4)G_{Qd}^2]/(G_{Ep})^2$ (experimental) versus q.

analyzed in the same way for the ratio of neutron to proton magnetic form factors. We find the values listed in Table VII.

IV. CORRECTIONS AND ERROR ANALYSIS

For the CD_2 experiments, errors and corrections have already been published.[11] Here we present only corrections and errors of the ratio measurements.

Table VIII lists the corrections made to the hydrogen and deuteron data before extraction of data. In Table IX we list the errors considered. All other errors are thought to be negligible ($<0.1\%$). We have assigned these errors as follows:

(1) Energy: 0.50% absolute calibration based on floating-wire measurements.

(2) Angle: ± 0.002 rad, the error being dependent on the scattering angle.

(3) Beam current: The Faraday cup is supposed perfect and the error in the secondary-emission monitor is assigned as $\frac{1}{2}$ the observed deviation between two calibrations.

TABLE VII. Liquid-target results: Magnetic deuteron and neutron form factors.

q^2 (F^{-2})	$(G_{Md}/G_p)^2$	$\dfrac{G_{Md}}{\mu_d[G_{Ed}^2+(q^4/18M_d^4)G_{Qd}^2]^{1/2}}$	$\left(\dfrac{G_{Mn}}{\mu_n}\right)\Big/\left(\dfrac{G_{Mp}}{\mu_p}\right)$
1.351	1.054 ± 0.200	1.09 ± 0.09	0.97 ± 0.04
1.964	$1.08\ \pm0.09$	1.08 ± 0.09	0.97 ± 0.03

(4) Beam position: ± 1 mm laterally and vertically, the error assigned depending on the scattering angle.

The other errors are self-explanatory.

V. DISCUSSION

A. Electric Scattering

Considering the results on G_{En} as a whole, i.e., both the solid and liquid targets, we seem to find a slight systematic difference, the solid-target points seeming to give slightly larger values than the liquid target. Although probably not significant, the difference, which could be attributed to many sources, is most certainly a manifestation of the fact that the errors encountered in a precise experiment are not normally distributed and the statistical addition is to some extent invalid. We conclude from our points alone that G_{En} is zero or slightly positive and seems to deviate from the extrapolated neutron-electron interaction. This deviation is perhaps due to the theoretical uncertainties in the deuteron form factors. Negative values of G_{En} at low q^2 seem definitely excluded.

In Fig. 3 we have plotted the results of this experiment and that of Drickey and Hand. We show here the measurement of $[G_{Ed}^2+(q^4/18M_d^4)G_{Qd}^2]/G_{Ep}^2$ with accompanying error, and we show two theoretical curves for the same quantity supposing $G_{En}=0$, the first being from the Hamada potential and the second from that of Glendenning and Kramer (No. 8).

TABLE VIII. Liquid target: Corrections; ΔE is the aperture of the analyzing slits.

θ in deg	65		70		135		85			135		145	
target	D_2	H_2	D_2	H_2	D_2	H_2	D_2	H_2	H_2	D_2	H_2	D_2	H_2
ΔE (MeV)	1.64	1.60	1.50	1.47	1.60	1.47	1.49	1.42	1.48	1.50	1.17	1.20	1.17
Bremsstrahlung	1.034	1.031	1.040	1.036	1.033	1.035	1.045	1.041	1.041	1.035	1.033	1.035	1.030
Ionization	1.025	1.022	1.028	1.025	1.024	1.023	1.033	1.030	1.028	1.026	1.028	1.030	1.026
Radiative corrections	1.170	1.176	1.215	1.216	1.184	1.778	1.224	1.222	1.223	1.204	1.205	1.215	1.202
Other corrections	0.990	···	···	···	···	···	0.983	···	···	···	···	···	···

The experimental points have a tendency to lie slightly above the curve, indicating a positive value of G_{En}. Secondly, one can see that the conclusions are influenced even by this choice of two very similar potentials. However, the choice of any potential currently regarded as a reasonable description of the deuteron seems unable to change the conclusion that a deviation from the linear extrapolation of the neutron-electron interaction is observed.

TABLE IX. Liquid target: errors in %.

θ in deg		65	70	135	85	135	145
q^2 deuteron in F^{-2}		0.606	1.302	1.411	1.890	2.035	1.963
Energy calibration		0.4	0.9	1.0	1.3	1.3	1.3
Angle		1.1	1.2	1.6	1.2	1.9	2.3
Monitoring	D_2	1.0	0.5	···	0.2	···	···
	H_2	1.0	0.5	0.7	0.5	0.3	0.7
Statistics	D_2	0.7	0.5	1.0	0.7	1.0	1.5
	H_2	0.8	0.8	0.9	0.6	0.9	1.3
Energy determination		0.5	0.4	0.8	0.3	0.7	0.7
Density ratio		0.5	0.5	0.5	0.5	0.5	0.5
Errors of geometry		0.3	0.3	0.3	0.4	0.6	0.8
Position of the beam	lateral	0.3	0.7	0.7	0.5	0.9	1.4
	vertical	0.5	0.5	0.5	0.5	0.5	0.5
Inelastic scattering		···	···	···	0.7	···	1.0
Errors in the corrections		0.5	0.5	0.5	0.5	0.5	0.5
Total error on the deuteron-proton ratio		2.4	2.2	2.8	2.3	3.1	4.0

B. Magnetic Scattering

Although these low-q^2 measurements are somewhat insensitive to magnetic scattering from the deuteron, we find the magnetic scattering to be greater than that naïvely expected from the $q^2=0$ normalization. Even if this could be caused by a failure in the theory, we are led to conclude that the ratio of form factors $(G_{Mn}/1.91)/(G_{Mp}/2.29)$ is less than 1 or almost 1 in this q^2 region.

VI. CONCLUSION

In conclusion, these results show that elastic electron-deuteron scattering gives very small values of G_{En} at small q^2, as predicted by the neutron-electron interaction, and that $G_{Mn}/1.91$ is very near $G_{Mp}/2.29$, in agreement with the inelastic-scattering measurements at higher transfers.[27]

[27] B. Grossetête, S. Jullian, and P. Lehmann, following paper, Phys. Rev. 141, 1435 (1966).